Performance and Scaling of Collaborative Sensing and Networking for Automated Driving Applications

Yicong Wang*, Gustavo de Veciana*, Takayuki Shimizu†, and Hongsheng Lu†

*Department of Electrical and Computer Engineering, The University of Texas at Austin
†TOYOTA InfoTechnology Center, U.S.A., Inc., Mountain View, CA

***Abstract*—A critical requirement for automated driving systems is enabling situational awareness in dynamically changing environments. To that end vehicles will be equipped with diverse sensors, e.g., LIDAR, cameras, (mmWave) radar, etc. Unfortunately the sensing 'coverage' and 'reliability' of a single vehicle is limited by environmental obstructions, e.g., other vehicles, buildings, people, objects etc. A possible solution is to adopt collaborative sensing amongst vehicles possibly assisted by infrastructure. This paper introduces new models and performance scaling analysis for vehicular collaborative sensing and networking. In particular, coverage and reliability gains are quantified, as are their dependence on the penetration of collaborative vehicles. We also evaluate the associated communication loads in terms of the V2V and/or V2I capacity requirements and how these depend on penetration. Collaborative sensing is shown to greatly improve sensing performance, e.g., improves coverage from 20% to 80% with a 20% penetration. In scenarios with limited penetration and enhanced reliability requirements, infrastructure can be used to sense the environment and relay data. Once penetration is high enough, sensing vehicles provide good coverage and data traffic can be effectively 'offloaded' to V2V connectivity, making V2I resources available to support other in-car services.**

I. Introduction

In future automated driving systems, vehicles will need to maintain real-time situational awareness in dynamically changing environments. Despite vehicles being equipped with multiple sensors, e.g., radar, LIDAR and cameras etc., the sensing 'coverage' and 'reliability' of a single vehicle is limited. Indeed such sensors typically rely on a Line-Of-Sight (LOS) to detect and track objects, so their performance is fragile in obstructed environments, e.g., a vehicle may have limited visibility of what is happening several cars ahead of it, and that information could be critical for path planning or determining car-following distance etc. Further without access to diverse points of view of an object, it may be difficult to recognize what it is, e.g., a cyclist viewed only from the front may look like a pedestrian.

To overcome this problem researchers and industry are considering enabling *distributed collaborative sensing* amongst neighboring vehicles, and possibly infrastructure, e.g., Road Side Units (RSUs) and/or base stations. The idea is to enable automated vehicles and/or RSUs to exchange High Definition (HD) and/or processed data to enhance situational awareness, see e.g., [1][2]. The benefits of this approach will depend on the penetration of collaborating vehicles/RSUs as well as obstructions in the environment. The communication loads can also be high and will need to be met by enabling new forms of connectivity.

Collaborative sensing is likely to be one of key requirements for automated driving [2], which is one of three most important use cases of emerging 5G systems [3]. Thus a basic understanding of sensing performance and traffic scaling is of great interest. This may involve substantial data rates per vehicle, e.g., 53 Mbps, for highly automated driving, and require low end-to-end delays, e.g., 100 ms or less depending on the application [4]. At high vehicle densities realizing such data exchanges via Vehicle-to-Infrastructure (V2I) resources is not likely to be possible, e.g., there could be tens to hundreds of vehicles sharing a base station. A possible solution is to leverage direct data exchanges amongst vehicles. In particular short range millimeter wave (mmWave) based LOS Vehicle-to-Vehicle (V2V) links can support exceedingly high data rates [5]. Unfortunately such links are also susceptible to obstructions, and thus, not unlike collaborative sensing itself, the capacity of such V2V networks is limited by the penetration of vehicles with such communication capabilities and obstructions in the environment. Thus in order to be viable (and reliable) collaborative sensing applications will leverage a mix of V2V and V2I connectivity, likely attempting to offload as much traffic as possible onto the V2V network links.

The aim of this paper is to develop initial models and analysis of the benefits, communication loads and requirements for vehicular collaborative sensing and networking. We focus on two intertwined classes of questions:

1. What are simple and tractable metrics for collaborative sensing performance in obstructed environments? How does performance scale in the penetration of collaborating vehicles and density of obstructions?

2. What are the network connectivity-capacity requirements to support collaborative sensing on V2V/V2I networks as a function of the penetration and density of vehicles?

Note that while our focus will be on vehicular networks, other distributed autonomous systems built on wireless systems share similar characteristics, including, e.g., robotic or possibly emerging aerial drone applications.

Contributions. The key contributions of paper are as follows.

- We introduce a new stochastic geometric model for collaborative sensing in obstructed environments with associated performance metrics capturing coverage and

reliability.
- We quantify the performance of collaborative sensing for varying reliability requirements, vehicle/object densities and penetrations of collaborative sensing vehicles.
- We study the performance and communication capacity requirements of sensing and communication architectures combining vehicles and infrastructures. revealing the critical role of infrastructure assistance in improving sensing coverage and communication reliability especially at the early stages of collaborative sensing with low penetration.

Related work. Vehicles can exchange real time sensor information with other vehicles/RSUs to enhance their view of an obstructed environment [6][7][8]. Currently available communication protocols, e.g., Dedicated Short-Range Communication (DSRC) and LTE, provide limited capacity for such exchange. Various use cases and requirements for different sensing technologies have been defined [4][9], and mmWave technology is being considered to support the sharing of HD sensor data [5][10]. [10] also compares different sensing and communication technologies. The capacity of Vehicular Ad Hoc Networks (VANET) has been studied in a variety of works, see e.g., [11][12][13], yet these do not consider the role of obstructions on mmWave channels. To our knowledge, our exploration on modeling and assessing the scaling and performance of collaborative sensing is novel, and the analysis of the evolution of network requirements with penetration has not been done before.

Organization. We begin by proposing a 2D model for sensing in obstructed environments in Section II. We then quantify the benefits that collaborative sensing would afford in terms of sensing redundancy and coverage in Section III. In Section IV we analyze the capacity requirements on V2V and V2I networks. We conclude the paper in Section V.

II. Modeling Collaborative Sensing in Obstructed Environments

We begin by introducing a simple stochastic geometric model to study the character of collaborative sensing.

A. Obstructed Environments and Sensing Capabilities

The environment includes all objects, i.e., vehicles, pedestrians, buildings, etc. In some settings there may be substantial a priori knowledge regarding the environment, e.g., static elements that are part of previously computed HD maps [14]. While the presence of such objects is already known they still impact collaborative sensing as they can obstruct a sensor's field of view, e.g., a building may obstruct a vehicle's view when entering an intersection. For simplicity we shall not differentiate among static and dynamic objects, and focus on sensing based on a snapshot in time[1].

The centers of objects are located on 2-D plane according to a Homogeneous Poisson Point Process (HPPP) Φ with intensity λ, i.e.,

$$\Phi = \{X_i | X_i \in \mathbb{R}^2,\ i = \mathbb{N}^+\} \sim \text{HPPP}(\lambda),$$

where X_i is the location of object i, and $\mathbb{N}^+$ is the set of positive integers. Each object, say i, has a shape modeled by a random closed convex set denoted $A_i \subset \mathbb{R}^2$ referenced to the origin 0 and independent of X_i. We let E_i denote the region it occupies which is given by

$$E_i = \{X_i\} \oplus A_i \triangleq \{X_i + x | x \in A_i\},$$

i.e., the object's shape A_i shifted to its location X_i, where $\oplus$ is the Minkowski sum, see Fig. 1a. Thus $E = \overset{\infty}{\underset{i=1}{\cup}} E_i$ denotes the region occupied by objects in the environment. We refer to the region not occupied by objects, $E^c = \{x | x \notin E\}$, as the *void space*. Fig. 1b illustrates our model for the environment.

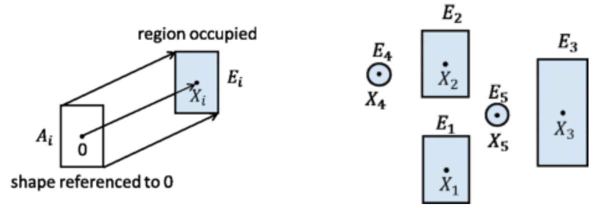

(a) Model for object i. (b) Model for environment.

Fig. 1. Model for environment based on randomly located and shaped objects.

It is unavoidable that as automated driving technologies are progressively introduced, only a fraction of vehicles will be equipped with sensors and/or participate in collaborative sensing. Thus only the subset equipped with sensors can participate in collaborative sensing – we shall refer to such objects as sensors. Each object has an independent probability p_s of being a sensor. Thus the locations of sensors, Φ^s, correspond to an independent thinning [16] of Φ, and $\Phi^s \sim$HPPP(λ^s) where $\lambda_s = p_s\lambda$. For a sensing object i, we assume for simplicity that there is *one* sensor located at the center. The sensor has a disc shaped sensing support $S_i^0 = b(0, R_i) \subset \mathbb{R}^2$ referenced to X_i, where R_i is the maximum radius of sensing, $b(0, R_i)$ is a disc centered at 0 with radius R_i. Sensor i can view any location in $X_i \oplus S_i^0$ if the location is not obstructed. We denote by $S_i = X_i \oplus S_i^0$ the sensing support of sensor i [2]

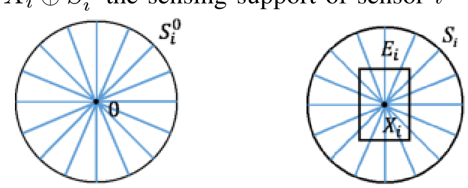

(a) S_i^0 (b) S_i

Fig. 2. Sensing support of sensor i, $S_i = S_i^0 \oplus X_i$.

Fig. 2 illustrates an example of a sensor's radial sensing support. The environment and the sensing field are thus modeled by an Independently Marked PPP (IMPPP), $\tilde{\Phi}$, which associates independent marks $M_i = (A_i, S_i^0)$ to each object i, i.e.,

$$\tilde{\Phi} = \big\{\big(X_i, M_i\big), i \in \mathbb{N}^+\big\}.$$

The aim is to model all the objects in the environment, including vehicles, pedestrians, motorcycles, buildings, etc.,

[1]In practice collaborative sensing system will track objects over time. Thus taking the snapshot point of view can be considered "worst case" assumption. Collaboration with oncoming crossroad vehicles and/or RSUs can improve sensing but has higher demand on communication, see [15] for more details.

[2]Our model and results can be easily generalized, i.e., sensors not located at centers and/or having different sensing support, or 3-D models.

thus we use a generalized HPPP model for the objects. Note in practice vehicles follow the lanes on roads or parking lots, yet the analysis for such settings is similar to the simplified setting we consider. Furthermore comparisons via simulation of a detailed highway model validate that the proposed HPPP model is a good approximation to study the performance of sensing in different scenarios. Our model may also apply to other (collaborative) sensing systems relying on wireless communication, while the model and analysis in this paper would focus on the unique characters of vehicular sensing, i.e., vehicles play the role of sensor, obstruction, and objects of interest at the same time.

B. Model for Vehicle's Region of Interest

We shall assume each sensing vehicle is interested in information within a certain range around it – usually measured in time, e.g., t_{interest} sec. The actual spatial range depends on the vehicle's speed s and is given by $s \cdot t_{\text{interest}}$. We model a sensing vehicle i's *region of interest*, D_i, as a disc, $b(X_i, r)$, centered at X_i with radius $r = s \cdot t_{\text{interest}}$. For a vehicle located at the center of a multi-lane road, its region of interest can be approximated by a rectangular set $[-s \cdot t_{\text{interest}}, \quad s \cdot t_{\text{interest}}] \times [-\frac{w_{\text{road}}}{2}, \frac{w_{\text{road}}}{2}]$, where w_{road} denotes the width of the road.

C. Collaborative Sensing in an Obstructed Environment

Next we define a sensor's coverage set given the environment and sensor model $\tilde{\Phi}$ as follows – see Fig. 3.

Definition 1. (Sensor coverage set) For sensor i in the environment and sensor model $\tilde{\Phi}$, we let $E^{-i} = \bigcup_{j:j\neq i} E_j$ denote the environment excluding E_i. The *coverage set* of sensor i, $C_i(\tilde{\Phi})$, is given by

$$C_i(\tilde{\Phi}) = \{x \in S_i \big| x \in E_i \text{ or } l_{X_i,x} \cap E^{-i} \subseteq \{x\}\}, \qquad (1)$$

where $l_{y,z}$ denotes the closed line segment between $y, z \in \mathbb{R}^2$. The *coverage area* of sensor i is the area of its coverage set which we denote $|C_i(\tilde{\Phi})|$.

In the above definition, we assume that a sensor is aware of E_i, the space its associated object occupies, i.e. no "self blocking". Also $l_{X_i,x} \cap E^{-i} \subseteq \{x\}$ verifies that the LOS channel between the sensor at X_i and location x is not blocked by other objects. A location $x \in C_i(\tilde{\Phi})$ may be in the void space or on the perimeter/surface of an object. In summary the coverage set of sensor i represents the surrounding environment that it is able to view under environmental obstructions.

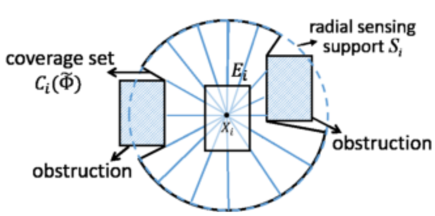

Fig. 3. Coverage set of sensor i in $\tilde{\Phi}$.

The expected coverage area of a *typical* sensor is given in the following theorem, where C^0 denotes the coverage set of a typical sensor shifted to the origin[3] and A^0 and S^0 are the associated shape and sensing support set referred to the location of the object. The set $S^0 \cap A^0$ denotes the region, if any, in the sensing support overlapping with the object, while $S^0 \backslash A^0 = \{x | x \in S^0, x \notin A^0\}$ is the region in the sensing support excluding the sensing object. Finally A denotes a random set with the same distribution as the shape of objects and is independent of A^0. Their distributions may be different, since the latter is conditioned on an environmental object being a sensor, i.e., being a sensing vehicle.

Theorem 1. *Under our environment and sensor model $\tilde{\Phi}$ the expected coverage area of a typical sensor is given by*

$$\mathrm{E}\big[|C^0|\big] = \mathrm{E}[|S^0 \cap A^0|] + \mathrm{E}\left[\int_{S^0\backslash A^0} e^{-\lambda \cdot \mathrm{E}[|l_{0,x} \oplus \check{A}|]} dx\right], \quad (2)$$

where $\check{A} = \{x | -x \in A\}$.

For example if objects are modeled as discs of radius r, i.e., $A = b(0, r)$, with probability 1, we have that $|l_{0,x} \oplus \check{A}| = \pi r^2 + 2r \cdot |x|$ (see [16]), so $\mathrm{E}\big[|C^0|\big]$ is straightforward to compute. The theorem shows how the coverage area of a *single* sensor decreases in the object density λ since the probability of sensing a given location (the term inside integral) decreases exponentially in λ. The proof leverages straightforward stochastic geometric results and is included in [15].

D. Sensor Coverage Area: Numerical and Simulation Results

Below we verify the robustness of our idealized analytical model by comparing to a simulation of vehicles on a freeway. For the analytical model, all objects (vehicles) are modeled as discs of radius $1.67\,\text{m}$, roughly corresponding to the footprint of a vehicle, and each has a sensing radius $100\,\text{m}$. For a typical vehicle i, we limit its region of interest and coverage set to a rectangular centered at X_i, $D_i = b(X_i, 100\,\text{m}) \cap ([-\infty, \infty] \times [X_i - 12\,\text{m}, X_i + 12\,\text{m}])$. This is geared at capturing the fact that vehicles are mainly interested in sensing nearby road and sidewalks and $12\,\text{m}$ is roughly the width of three lanes. Simulations are based on the highway scenario specified in [9] with 3 lanes in each direction of width 4 m each. Vehicles are placed on each lane following a linear Matérn process [17], i.e., randomly located but ensuring a minimum gap of 10m among the centers of vehicles on the same lane. Vehicles are modeled as 4.8m $\times$1.8m rectangles, and distance from the center locations to the lane center are uniformly distributed $\text{unif}[-1, 1]$m. The coverage area does not include the region off the road. Fig. 4 gives an example of sensing coverage in analytical model and highway simulation, which show similar characteristics.

Fig. 5a exhibits analytical and simulation results for a typical vehicle's coverage area normalized by the area of sensing support scales versus vehicle density λ. As can be seen the analytical and simulation results exhibit similar trends – sensor coverage area decreases with λ due to increased obstructions and becomes heavily limited at high vehicle densities, i.e., less

[3] Its distribution is formally referred to as the Palm distribution [16].

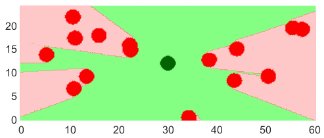

(a) analytical model

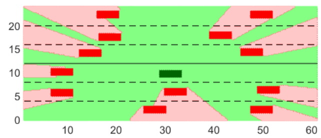

(b) highway simulation

Fig. 4. Sensing of a typical vehicle in (a) analytical model and (b) highway simulation model. The green shapes are reference objects, the red shapes are obstructions, light green represents sensed region, light red indicates obstructed region.

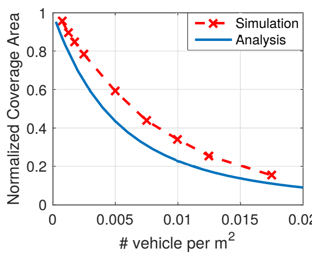

(a) coverage area

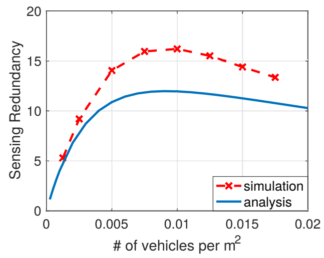

(b) sensing redundancy

Fig. 5. (a) normalized coverage area of a typical vehicle. (b) collaborative sensing redundancy of a typical vehicle.

than 20%. In an obstructed environment, collaborative sensing will be critical to achieve better coverage and reliability for each vehicle's region of interest. We consider this next.

III. Benefits of Collaborative Sensing

The benefits of collaborative sensing are twofold: (1) it increases sensing redundancy/diversity leading to improved reliability, and (2) it improves coverage and extends sensing range. We consider two metrics for the performance of collaborative sensing, i.e., *redundancy* and *coverage*. In this paper we focus on sensing void locations, i.e., where there is no object and vehicles may move to. We can similarly study the sensing of objects, yet the analysis and results are similar.

Sensing redundancy. We define sensing redundancy as the number of collaborative sensing vehicles that can view a location – higher sensing redundancy provides greater reliability and robustness to sensor/communication link failures.

Definition 2. (Sensing redundancy) Given an environment and sensing field, $\tilde{\Phi}$, and a subset of sensors $K \subseteq \Phi^s$ which are collaborating, the *sensing redundancy for a location* x is the number of sensors in K that view x, denoted by

$$R(\tilde{\Phi}, K, x) = \sum_{i: X_i \in K} \mathbb{1}\left(x \in C_i(\tilde{\Phi})\right). \qquad (3)$$

The expected redundancy of a location in the void space is then given by the following theorem.

Theorem 2. *Given an environment and sensing field $\tilde{\Phi}$ and all sensors collaborate, $K = \Phi^s$, the expected redundancy given for a typical location x in the void space is*

$$\mathrm{E}[R(\tilde{\Phi}, \Phi^s, x) | x \notin E] = \frac{p_s \cdot \lambda \cdot \mathrm{E}[|C^0 \backslash A^0|]}{e^{-\lambda \cdot \mathrm{E}[|A|]}}, \qquad (4)$$

where $\mathrm{E}[|C^0 \backslash A^0|]$ *is given in Eq. 2.*

The proof follows from the definition of redundancy and coverage set and is included in [15]. Fig. 5b exhibits the expected sensing redundancy of a typical location in the void space. As can be gleaned from our analytical results, sensing redundancy for a location is proportional to p_s so we only exhibit results for $p_s = 1$. At small densities sensors are not likely to be blocked thus redundancy first increases in the density of objects λ. However, at higher densities, the objects obstruct each other reducing the coverage area of each sensor and the resulting reduced sensing redundancy. The simulation results show the expected redundancy of a random location in the central two lanes, and exhibit similar trends as the analysis. Overall one can conclude that collaborative sensing will provide highest redundancy at moderate densities, i.e., this is where in principle collaborative sensing is most reliable and robust to sensor/communication failures.

Collaborative sensing coverage. A location in a vehicle's region of interest is covered by collaborative sensing if the location can be reliably sensed, i.e., sensed by a sufficient number of collaborating sensors. We define the collaborative sensing coverage and reliability for a vehicle as follows.

Definition 3. (Collaborative sensing coverage and reliability) Given an environment and sensing field $\tilde{\Phi}$, a minimum redundancy requirement $\gamma \in \mathbb{N}^+$ for reliable sensing of a location, a subset of collaborating sensors, $K \subseteq \Phi^s$, and sensor i's region of interest D_i, the *γ-coverage set* of sensor i is the region within its region of interest, which is sensed by at least γ sensors in K, denoted by

$$C_c(\tilde{\Phi}, K, D_i, \gamma) \triangleq \left\{x \middle| x \in D_i, R(\tilde{\Phi}, K, x) \geq \gamma\right\}. \qquad (5)$$

The *γ-coverage* of sensor i is the area of the γ-coverage set, $|C_c(\tilde{\Phi}, K, D_i, \gamma)|$. The *$\gamma$-coverage reliability* is fraction of D_i that is reliably sensed, $|C_c(\tilde{\Phi}, K, D_i, \gamma)|/|D_i|$.

Denote by D^0 the possibly random (may depend on s) region of interest associated with a typical sensing vehicle, $A^s \subset \mathbb{R}^2$ a random set having the same distribution of the shape of sensors. The expected 1-coverage can then be approximated by

$$\begin{aligned}
&\mathrm{E}\left[|C_c(\tilde{\Phi}, \Phi^s, D^0, 1)|\right] \approx \\
&\quad \mathrm{E}[|D^0 \cap C^0|] + \mathrm{E}[|D^0 \backslash (C^0 \cap A^0)|] \cdot (1 - e^{-\lambda^s \mathrm{E}[|A^s|]}) \\
&\quad + \left(\mathrm{E}[|D^0 \backslash A^0|] \cdot e^{-\lambda \mathrm{E}[|A|]} - \mathrm{E}[|D^0 \cap C^0 \backslash A^0|]\right) \\
&\quad \cdot (1 - e^{-\mathrm{E}[R(\tilde{\Phi}, \Phi^s, x) | x \notin E]}). \qquad (6)
\end{aligned}$$

This approximation is based on decomposing D^0 into various sets: $D^0 \cap C^0$ is the set covered by the sensor. In the region not covered by the sensor, we have $D^0 \cap E \backslash C^0$ the set occupied by objects and $D^0 \backslash (E \cup C^0)$ the void space. The collaborative coverage in each set can then be evaluated as follows, $\mathrm{E}[|D^0 \cap C^0|]$ is area sensed by the vehicle itself, $\mathrm{E}[|D^0 \backslash (C^0 \cap A^0)|] \cdot (1 - e^{-\lambda^s \mathrm{E}[|A^s|]})$ the area of region not covered by the sensor but occupied by other sensing vehicle bodies and sensed through collaboration, $\left(\mathrm{E}[|D^0 \backslash A^0|] \cdot e^{-\lambda \mathrm{E}[|A|]} - \mathrm{E}[|D^0 \cap C^0 \backslash A^0|]\right)$ is the area of void space not covered by the sensor and $1 - e^{-\mathrm{E}[R(\tilde{\Phi}, \Phi^s, x) | x \notin E]}$ is an approximation for the probability a void location is sensed via collaboration assuming the redundancy of a void location has a Poisson distribution with a mean given in Thm. 2. A more general approximation for $\gamma \geq 1$ coverage is in [15].

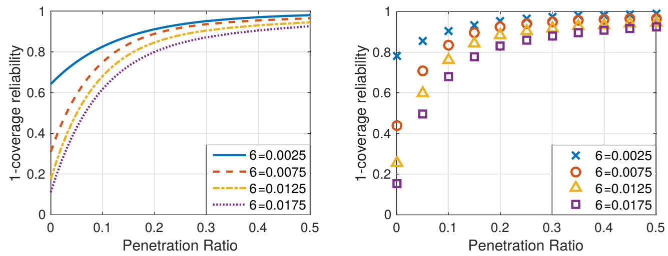

(a) Analysis (b) Simulation

Fig. 6. 1-coverage reliability: (a) based on analytical approximation in Eq. 6, and (b) obtained by simulation of highway scenario.

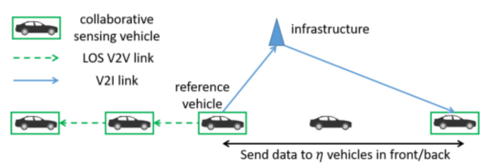

Fig. 7. Collaborative sensing of vehicles in a single lane with V2V + V2I network. Vehicle uses V2I to relay data when LOS V2V links are blocked.

Fig. 6 exhibits the expected 1-coverage reliability for varying penetrations p_s and vehicle densities λ. The highway simulation results show the same trends as our analytical results. Note that Eq. 6 is an approximation of the analytical model, which is different from our simulation of the highway scenario. As expected, reliability increases monotonically in p_s. More importantly, collaborative sensing can greatly improve reliability even with a small penetration of collaborating vehicles, e.g., over 0.8 reliability when 20% of vehicles collaborate as compared to 0.2 reliability without collaboration at a vehicle density $\lambda = 0.0175/\mathrm{m}^2$. Such results indicate that it can be beneficial to share sensor data even with only a subset of neighboring vehicles. However to guarantee high reliability, deploying sensing infrastructure may be necessary, especially at low penetrations.

IV. Network Capacity Scaling for Collaborative Sensing Applications

In this section we study the network capacity requirements for collaborative sensing. We envisage both V2V and V2I connectivity would be available. Vehicles would primarily use (mmWave) LOS V2V links to share data due to the high data rate. V2I could serve as fallback as mmWave V2V links/paths may be blocked/unavailable, in particular when penetration is limited during the transition from legacy systems. Below we study how V2I and V2V capacity requirements scale with penetration p_s. Our analysis provides a comprehensive view of a possible evolution of future network capacity requirements.

We first consider a vehicle located on a single lane road with a penetration p_s. The gap between two neighboring vehicles is t_{gap}. A sensing vehicle generates sensor data at rate ν, and needs to send data to $\eta = \lfloor \frac{t_{\mathrm{interest}}}{t_{\mathrm{gap}}} \rfloor$ other vehicles in front and behind it, see Fig. 7. A vehicle has LOS V2V communication channels to the neighboring vehicles in front and back. A non collaborating vehicle thus blocks the V2V relay path along the chain of vehicles. If a LOS V2V relay path is not available, we assume the reference vehicle relays data through

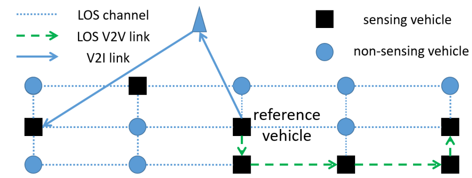

Fig. 8. Collaborative sensing of vehicles in a single lane using V2V + V2I, with V2V relay assistance from vehicles in the two neighboring lanes.

the infrastructure and the receiving vehicle can then further relay data to upstream/downstream or vehicles via available V2V links. Let N_{UL} and $N_{\mathrm{DL}}^{\mathrm{U}}$ be random variables denoting the number of uplink and unicast downlink V2I transmissions required by a sensing vehicle. The expected required V2I uplink capacity c_{UL} and V2I downlink capacity for broadcast, $c_{\mathrm{DL}}^{\mathrm{B}}$, and unicast, $c_{\mathrm{DL}}^{\mathrm{U}}$, are given in the following theorem.

Theorem 3. *Under the single lane model, the density of vehicles is λ_{v}, each sensing vehicle generates data at rate ν and shares with $\eta = \lfloor t_{\mathrm{interest}}/t_{\mathrm{gap}} \rfloor$ vehicles in front and back. The V2I capacity requirements on a infrastructure serving the linear road segment of length $d\,\mathrm{m}$ are given by*

$$c_{\mathrm{UL}} = c_{\mathrm{DL}}^{\mathrm{B}} = p_s \cdot \lambda_{\mathrm{v}} \cdot d \cdot \mathrm{E}[N_{\mathrm{UL}}] \cdot \nu, \tag{7}$$

$$c_{\mathrm{DL}}^{\mathrm{U}} = p_s \cdot \lambda_{\mathrm{v}} \cdot d \cdot \mathrm{E}[N_{\mathrm{DL}}^{\mathrm{U}}] \cdot \nu, \tag{8}$$

where

$$\mathrm{E}[N_{\mathrm{UL}}] = 1 - \Big(\sum_{k=0}^{\eta} p_s^k \cdot (1-p_s)^{\eta-k}\Big)^2, \tag{9}$$

$$\mathrm{E}[N_{\mathrm{DL}}^{\mathrm{U}}] = \begin{cases} 2(\eta-1)p_s(1-p_s), & \text{if } \eta \geq 2, \\ 0, & \text{otherwise} \end{cases}. \tag{10}$$

The proof of is included in [15]. The above results convey the *average* capacity requirements on V2I infrastructure. Unfortunately a single non-collaborating vehicle can block the V2V LOS links amongst a large number of vehicles and result in a *burst* of V2I traffic especially at high penetrations, e.g., when vehicles in front and back of the non-collaborating vehicle are all collaborating. The required V2I capacity to handle such bursts can thus be much higher.

The single lane relaying scenario studied above is a worst case, i.e., data can only be relayed by vehicles on the same lane. One can also consider scenarios where in addition collaborative vehicles on either of two neighboring lanes participate in V2V relaying. LOS links among vehicles on neighboring lanes are less likely to be blocked, but LOS links to distant vehicles in neighboring lanes will see larger path loss and may experience more interference, e.g., from transmissions of vehicles in the same lane. Thus for simplicity suppose vehicles only communicate with the closest vehicle in a neighboring lane and consider the simple grid connectivity model shown in Fig. 8. Each node on the grid corresponds to a vehicle, and each row represents a lane. Vehicles have LOS channels to neighboring vehicles on the grid. For comparison purposes we suppose, as before, that the reference vehicle needs to send data to η vehicles in front and back in the *same* lane. Vehicles can receive data via V2V links if there is an LOS V2V relay path on the grid. To limit the number of hops and associated

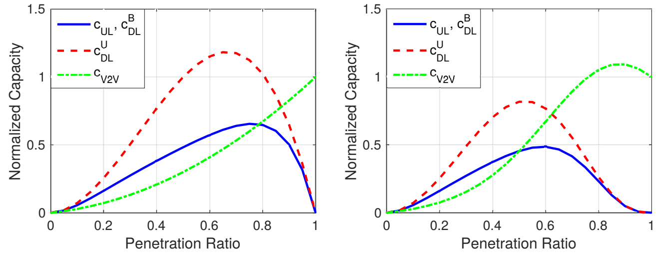

(a) Single lane

(b) Single lane assisted by neighbors

Fig. 9. How V2I capacity requirements, normalized by $\lambda_{\mathrm{v}} \cdot d \cdot \nu$, scale with p_s in (a) single lane and (b) single lane assisted by vehicles in neighbor lanes. c_{UL} is uplink capacity, $c_{\mathrm{DL}}^{\mathrm{B}}$ and $c_{\mathrm{DL}}^{\mathrm{U}}$ are downlink capacity using broadcast and unicast. c_{V2V} is V2V throughput per sensing vehicle normalized by the V2V throughput at full penetration, $p_s = 1$.

delays, we assume that a relay path can not include links in *both* forward and backward directions.

Based on this model, whether vehicles in the $(k+1)^{th}$ column from the reference vehicle can receive data via V2V links depends on whether the vehicles in the $(k+1)^{th}$ column are collaborating and can get data from vehicles in the k^{th} column. In this setting one can again compute the expected V2I capacity requirements to deliver data to vehicles in each column and thus the total capacity requirements as a function of η and p_s. – a detailed analysis is included in [15].

A. Numerical Results

Fig. 9 exhibits how the V2I capacity, c_{UL}, $c_{\mathrm{DL}}^{\mathrm{B}}$ and $c_{\mathrm{DL}}^{\mathrm{U}}$, normalized by $\lambda_{\mathrm{v}} \cdot d \cdot \nu$ and the average V2V throughput per sensing vehicle (normalized by c_{V2V} at $p_s = 1$), vary with p_s in single lane and single lane assisted by vehicles in neighboring lanes scenarios. The results correspond to the case where $\eta = 5$, i.e., vehicles have $10\,\mathrm{sec}$ prediction of the environment ($t_{\mathrm{gap}} = 2\,\mathrm{sec}$). An increase in p_s causes more vehicles to send/receive data, but also results in improved V2V connectivity. When p_s is small, both the number of collaborative sensing vehicles and the capacity per sensing vehicle increase with p_s, thus V2I traffic increases. At higher penetrations, V2V connectivity improves and the V2I capacity requirements of a sensing vehicle decreases, resulting in lower and eventually negligible V2I traffic. Comparing the results with and without assistance from vehicles in neighboring lanes, we observe, as expected, that V2I traffic is smaller when vehicles in neighboring lanes help relay data, while higher V2V throughput is required.

In summary the V2I traffic resulting from collaborative sensing data exchanges would be highest at intermediate penetrations, e.g., ranging from 0.5 to 0.7, but eventually would decline once most vehicles participate in both collaborative sensing and V2V networking. This suggests an evolution path where V2I resources are initially critical to safety-related services like collaborative sensing, but eventually at high penetrations of sensing vehicles, traffic can be effectively offloaded to V2V network, e.g., in the single lane assisted by neighboring lanes, $c_{\mathrm{UL}}, c_{\mathrm{DL}}^{\mathrm{B}}$ per vehicle is less than 0.25ν if $p_s > 0.8$, and the infrastructure may transition to supporting non-safety-related services, e.g., mobile high data rate entertainment and dynamic digital map update. These results are likely robust to improved models, yet more detailed analysis based on more accurate V2V mmWave channel and networking models would be needed to provide more accurate quantitative assessment.

V. Conclusion

Collaborative sensing can greatly improve a vehicle's sensing coverage and reliability, but suffers at low penetrations due to, both a lack of available collaborators, and blockages in (mmWave) V2V relaying paths. Access to V2I connectivity will thus be important to provide communication for collaborative sensing when V2V relaying paths are unavailable. At higher penetrations, the average V2I traffic is low, but the infrastructure should still have the ability to support traffic bursts when the V2V network becomes disconnected. Deploying sensing capable RSUs may provide good sensing coverage, yet sensing based only on RSUs might not provide enough sensing redundancy while the sensing capabilities of vehicles should clearly be leveraged. We see the eventual combination of vehicular and RSU based collaborative sensing as the most cost effective way to achieve high coverage and reliability for automated driving applications.

References

[1] S.-W. Kim, B. Qin *et al.*, "Multivehicle cooperative driving using cooperative perception: Design and experimental validation," *IEEE Trans. Intell. Transp. Syst.*, vol. 16, no. 2, pp. 663–680, 2015.

[2] L. Hobert, A. Festag *et al.*, "Enhancements of V2X communication in support of cooperative autonomous driving," *IEEE Commun. Mag.*, vol. 53, no. 12, pp. 64–70, 2015.

[3] "5G automotive vision," *5GPPP white paper*, October 2015.

[4] "3GPP TS 22.186 v15.1.0 study on enhancement of 3GPP support for V2X scenarios; stage 1 (release15)," June 2016.

[5] V. Va, T. Shimizu *et al.*, "Millimeter wave vehicular communications: A survey," *Foundations and Trends® in Networking*, vol. 10, no. 1, pp. 1–113, 2016.

[6] A. Rauch, F. Klanner *et al.*, "Car2x-based perception in a high-level fusion architecture for cooperative perception systems," in *Intelligent Vehicles Symposium (IV)*, 2012, pp. 270–275.

[7] S.-W. Kim, Z. J. Chong *et al.*, "Cooperative perception for autonomous vehicle control on the road: Motivation and experimental results," in *IROS*, 2013, pp. 5059–5066.

[8] X. Zhao, K. Mu *et al.*, "A cooperative vehicle-infrastructure based urban driving environment perception method using a D-S theory-based credibility map," *Optik-International Journal for Light and Electron Optics*, vol. 138, pp. 407–415, 2017.

[9] "3GPP TR 22.886 v15.1.0 study on enhancement of 3GPP support for 5G V2X services (release15)," March 2017.

[10] J. Choi, V. Va *et al.*, "Millimeter-wave vehicular communication to support massive automotive sensing," *IEEE Commun. Mag.*, vol. 54, no. 12, pp. 160–167, 2016.

[11] G. Zhang, Y. Xu *et al.*, "Multicast capacity for VANETs with directional antenna and delay constraint," *IEEE J. Sel. Areas Commun.*, vol. 30, no. 4, pp. 818–833, 2012.

[12] S. Kwon, Y. Kim *et al.*, "Analysis of connectivity and capacity in 1-D vehicle-to-vehicle networks," *IEEE Trans. Wireless Commun.*, vol. 15, no. 12, pp. 8182–8194, 2016.

[13] X. He, H. Zhang *et al.*, "Transmission capacity analysis for linear VANET under physical model," *China Communications*, vol. 14, no. 3, pp. 97–107, 2017.

[14] H. G. Seif and X. Hu, "Autonomous driving in the iCity–HD maps as a key challenge of the automotive industry," *Engineering*, vol. 2, no. 2, pp. 159–162, 2016.

[15] Y. Wang, "Impact of blockage and mobility on collaborative sensing and millimeter wave based communication," 2017. [Online]. Available: http://users.ece.utexas.edu/ gustavo/phd-theses/Yicong.Wang2017.pdf

[16] S. N. Chiu, D. Stoyan *et al.*, *Stochastic geometry and its applications*. John Wiley & Sons, 2013.

[17] B. Matérn, *Spatial variation*. Springer Science & Business Media, 2013, vol. 36.